

Article

Dehydrogenation Kinetics and Modeling Studies of MgH₂ Enhanced by Transition Metal Oxide Catalysts Using Constant Pressure Thermodynamic Driving Forces

Saidi Temitope Sabitu and Andrew J. Goudy *

Department of Chemistry, Delaware State University, Dover, DE 19901, USA;

E-Mail: sabtemmy@yahoo.com

* Author to whom correspondence should be addressed; E-Mail: agoudy@desu.edu;

Tel.: +1-302-857-6534; Fax: +1-302-857-6539.

Received: 27 May 2012; in revised form: 13 June 2012 / Accepted: 14 June 2012 /

Published: 25 June 2012

Abstract: The influence of transition metal oxide catalysts (ZrO₂, CeO₂, Fe₃O₄ and Nb₂O₅) on the hydrogen desorption kinetics of MgH₂ was investigated using constant pressure thermodynamic driving forces in which the ratio of the equilibrium plateau pressure (p_m) to the opposing plateau (p_{op}) was the same in all the reactions studied. The results showed Nb₂O₅ to be vastly superior to other catalysts for improving the thermodynamics and kinetics of MgH₂. The modeling studies showed reaction at the phase boundary to be likely process controlling the reaction rates of all the systems studied.

Keywords: hydrogen storage; magnesium hydride; kinetics; modeling

1. Introduction

Magnesium hydride has received considerable attention as a promising hydrogen storage material for on-board vehicular applications because of its high theoretical hydrogen storage capacity (7.6 wt%) and high volumetric density (110 g/L) as well as low cost. However, its practical application is hindered by its high thermal stability and slow desorption kinetics [1–9]. Several attempts have been made to improve the thermodynamics and kinetics properties of MgH₂ by reducing the particle size via ball milling and alloying with other transition metals and their oxides [4,9–11]. Sohn and Enami [11] reported the loss of hydrogen capacity when transition metals are added to the MgH₂ system. They stated that only a small amount of these transition elements is needed to improve the reaction kinetics

and prevent a significant decrease in the hydrogen storage capacity of MgH_2 . Oelerich *et al.* [12] investigated the influence of metal oxides such as Sc_2O_3 , TiO_2 , V_2O_5 , Cr_2O_3 , Mn_2O_3 , Fe_3O_4 , CuO , Al_2O_3 and SiO_2 on the hydrogen sorption behavior of MgH_2 . They found that the composite material containing Fe_3O_4 showed the fastest desorption kinetics. They also reported that as little as 0.2 mol% of the catalysts is enough to provide fast sorption kinetics. Barkhordarian *et al.* [9] researched the efficiency of Nb_2O_5 as a catalyst for fast hydrogen absorption/desorption kinetics of magnesium and found the catalytic effect of Nb_2O_5 to be superior when compared to other metal and metal oxide catalysts for both absorption and desorption reactions. Subsequent studies [9] on the effect of varying Nb_2O_5 content on the hydrogen reaction kinetics of magnesium showed that fastest kinetics was obtained using 0.5 mol% of Nb_2O_5 and that the activation energy for hydrogen desorption reaction varies exponentially with Nb_2O_5 concentration. It should be noted that none of these kinetics studies attempted to compare the intrinsic reaction rates of catalyzed magnesium hydride systems using constant pressure thermodynamic driving forces. It is very important that this be done because without constant pressure driving forces, results will vary largely as the conditions change. The importance of this unique method was first demonstrated by Goudy and coworkers [13–15] when they analyzed the kinetic behavior of a series of LaNi_5 -based intermetallic hydrides. Since that time, they have used this technique to study the kinetics of other materials such as sodium alanate [16], MgH_2 [2], $\text{CaH}_2/\text{LiBH}_4$ [17] and $\text{LiNH}_2/\text{MgH}_2$ [18] systems. In this study, an attempt has been made to compare the intrinsic dehydriding kinetics of MgH_2 ball milled with various transition metal oxides using constant pressure thermodynamic driving forces. The results should provide more insight into the role that catalysts may have on reaction temperature and rates.

2. Experimental Section

The materials used in this research were obtained from Sigma Aldrich. The MgH_2 powder was hydrogen storage grade, and according to the information provided by the supplier, the total amount of trace metal contaminants was less than 0.1%. Sample handling, weighing and loading were performed in a Vacuum Atmospheres argon-filled glove box that was capable of achieving less than 1 ppm oxygen and moisture. Prior to analysis, each sample mixture was milled for up to 10 h in a SPEX 8000M Mixer/Mill that had an argon-filled stainless steel pot which contained four small stainless steel balls. Temperature Programmed Desorption (TPD) and Pressure Composition Isotherm (PCI) analyses were done in a gas reaction controller unit to evaluate the hydrogen desorption properties of each reaction mixture. This apparatus was manufactured by the Advanced Materials Corporation in Pittsburgh, PA. The unit was fully automated and was controlled by a Lab View-based software program. The TPD and PCI analyses were done on freshly ball-milled materials and no activation procedure was necessary. The TPD analyses were done in the 30–450 °C range at a temperature ramp of 4 °C/min. Thermal Gravimetric and Differential Thermal Analysis (TG/DTA) was conducted to determine the thermal stability of the mixtures using a Perkin Elmer Diamond TG/DTA. The experimental apparatus used to perform kinetics was made essentially of stainless steel and equipped with ports for adding hydrogen, venting and evacuating. Pressure regulators were installed to control the hydrogen pressure applied to the sample and to allow hydrogen to flow to or from the sample into a remote reservoir. A method that allowed samples to be measured at the same constant pressure driving

force was employed in order to compare the kinetics of the different samples. High purity hydrogen gas of 99.999% purity was used throughout the analyses.

3. Results and Discussion

3.1. Temperature Programmed Desorption Measurements

Temperature Programmed Desorption (TPD) measurements were done on several ball milled mixtures of MgH_2 with 4 mol% of Nb_2O_5 , ZrO_2 , CeO_2 and Fe_3O_4 . The samples were ball milled for 10 h and their thermal desorption performance was studied to determine the temperature at which hydrogen was released from the sample mixtures. By so doing, we can understand the effect of each catalyst on the hydrogen desorption properties of MgH_2 . It can be seen from the desorption curves shown in Figure 1 that MgH_2 has the highest onset temperature of about 310 °C and that the catalyzed samples have lower desorption temperatures. The mixture of $\text{MgH}_2 + \text{Fe}_3\text{O}_4$ has the lowest onset desorption temperature of about 200 °C. The onset temperature of the reacting mixtures are in the order: pure $\text{MgH}_2 > \text{CeO}_2 > \text{ZrO}_2 > \text{Nb}_2\text{O}_5 > \text{Fe}_3\text{O}_4$. The plot also revealed that all of the samples released less than 6 wt% of hydrogen. The reduction in hydrogen weight percentage is most likely due to the partial oxidation of the Mg in the alloy caused by the presence of oxide in all the transition metal oxide catalysts. These results confirm that the addition of transition metal oxide catalysts is effective in reducing the desorption temperature of MgH_2 , although accompanied with a small weight penalty. The values of the onset temperatures are summarized in Table 1.

Figure 1. Temperature Programmed Desorption (TPD) profiles for MgH_2 and catalyzed MgH_2 materials.

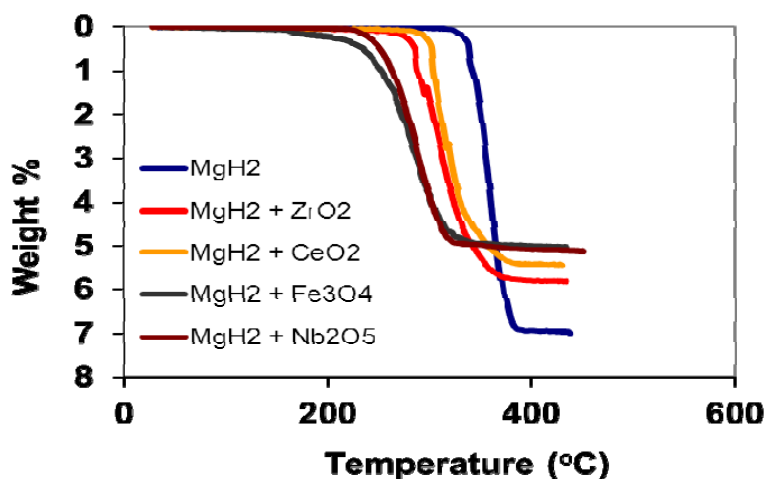


Table 1. Thermodynamic and kinetics parameters for catalyzed MgH_2 materials.

Sample	Onset Temperature/°C	$\Delta H/(\text{kJ/mol})$	T_{90}/min	$E_a/(\text{kJ/mol})$
MgH_2	310	78.8	32	174
$\text{MgH}_2 + 4 \text{ mol \% ZrO}_2$	260	75.2	21	140
$\text{MgH}_2 + 4 \text{ mol \% CeO}_2$	270	74.7	19	113
$\text{MgH}_2 + 4 \text{ mol \% Fe}_3\text{O}_4$	200	72.4	17	108
$\text{MgH}_2 + 4 \text{ mol \% Nb}_2\text{O}_5$	205	70.2	16	95

3.2. Programmed Composition Isotherm Measurements

Pressure Composition Isotherms were constructed for MgH_2 and the catalyzed MgH_2 mixtures. Figure 2 shows the desorption isotherms for these samples at 400 °C. It can be seen from the curves that the plateau pressures are about the same for all the samples. The data from these isotherms were used to construct the Van't Hoff plots shown in Figure 3. The reaction enthalpies for the mixtures were determined from the slopes of these plots and the values are summarized in Table 1. It is evident from the ΔH values that the thermodynamic stability of MgH_2 decreases with the addition of transition metal oxide catalysts.

Figure 2. Desorption isotherms for MgH_2 and catalyzed MgH_2 materials.

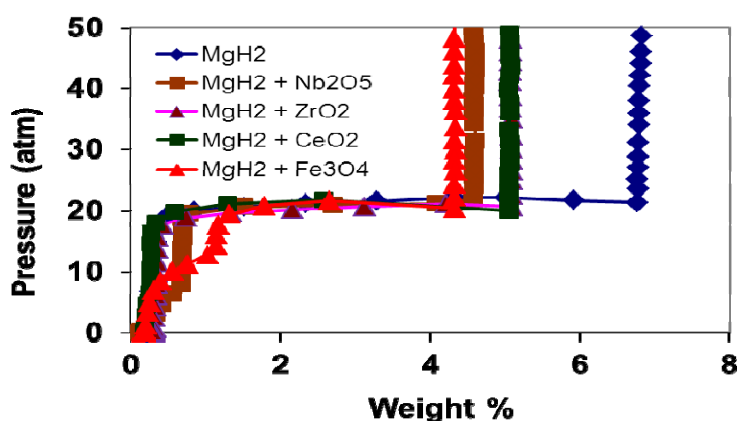
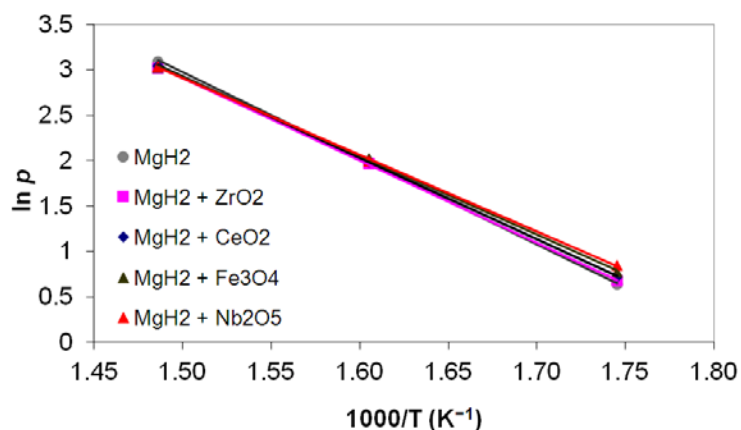


Figure 3. Van't Hoff desorption plots for MgH_2 and catalyzed MgH_2 materials.

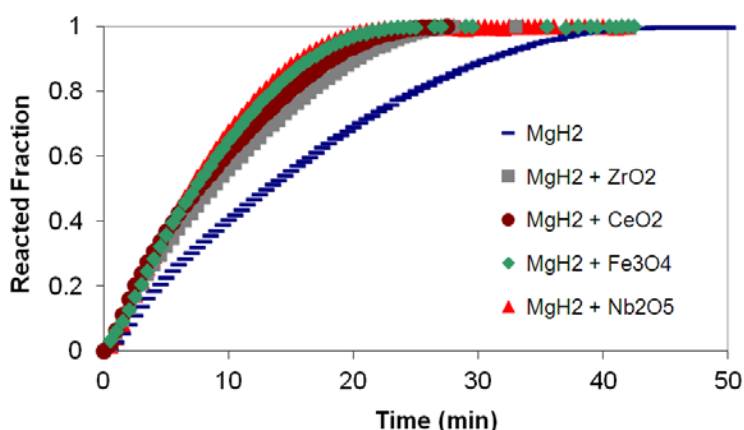


3.3. Kinetics Measurements

In addition to having a low desorption temperature, it is also important that samples have fast reaction rates. Desorption kinetics experiments were carried out on each sample at 400 °C to determine the catalytic effect of transition metal oxides on hydrogen desorption rates from MgH_2 . A novel concept of constant pressure thermodynamic driving force was used to achieve these desorption kinetics measurements. This was done by adjusting the hydrogen pressure in the reactor to a slightly higher value than that of the mid-plateau pressure (p_m), to ensure that only the hydrogen rich phase was present initially and sealing off the reactor. The pressure in the remaining system (p_{op}) was then

adjusted to a value such that the ratio between the mid-plateau pressure and the opposing pressure (p_m/p_{op}) was a small whole number. This ratio is defined as the N-value. In these experiments, the N-value was set at 5 for all the sample mixtures. The theoretical basis for using constant pressure thermodynamic forces is that the pressure ratio is proportional to ΔG (the Gibbs free energy). The proportionality can be expressed as: $\Delta G \approx RT \ln(p_m/p_{op})$. If the pressure ratio is the same then ΔG will be the same for all the reactions. Figure 4 contains plots of the reacted fraction versus the time for hydrogen desorption from the MgH_2 mixtures with and without catalysts. It can be seen that the uncatalyzed MgH_2 sample has the slowest hydrogen desorption rate. The addition of transition metal oxides improved the kinetics of MgH_2 with Nb_2O_5 and Fe_3O_4 having the fastest desorption reaction kinetics. The times required for all of these reactions to reach 90 percent completion (T_{90}) are summarized in Table 1.

Figure 4. Desorption kinetics for MgH_2 and catalyzed MgH_2 materials at 400 °C and $N = 5$.



3.4. Kinetics Modeling Studies

Smith and Goudy [15], while performing kinetics modeling studies on $LaNi_{5-x}Co_x$ hydride system ($x = 0, 1, 2$ and 3), reported two theoretical equations based on the shrinking core model that were successfully used to model the system. The equations are shown below:

$$\frac{t}{\tau} = 1 - (1 - X_B)^{1/3} \quad (1)$$

where $\tau = \frac{\rho_B R}{bk_s C_{Ag}}$

$$\frac{t}{\tau} = 1 - 3(1 - X_B)^{2/3} + 2(1 - X_B) \quad (2)$$

where $\tau = \frac{\rho_B R^2}{6bD_e C_{Ag}}$, t is the time at a specific point in the reaction, X_B is the fraction of the metal reacted. R is the initial radius of the hydride particles, b is a stoichiometric coefficient of the metal, C_{Ag} is the gas phase concentration of reactant, D_e is the effective diffusivity of hydrogen atoms in the hydride, ρ_B is the density of the metal hydride and k_s is a rate constant. It was found that a model based on Equation (1) will have chemical reaction at the phase boundary controlling the reaction rate. This is

called the shrinking particle model (SPM). A model based on Equation (2) is one in which the overall reaction rate is controlled by diffusion. Both models were applied to the current study to determine which kinetic model best describes the reactions. Equations (1) and (2) were fitted to the kinetic data for each of the reaction sample mixtures. Figures 5–9 each contain three curves. One is an experimental curve taken from the desorption kinetics curve shown in Figure 4, a second curve was calculated from the SCM with diffusion controlling the overall reaction and a third curve was calculated with chemical reaction at the phase boundary controlling the rate. In order to determine the theoretical curves, it was first necessary to determine a value for τ . It was not necessary to know the values of all the physical parameters in Equations (1) and (2) in order to do this. The determination of τ was accomplished through a series of statistical data analyses in which the value of τ necessary to minimize the standard deviation between the experimental and theoretical data was calculated. Thus τ was a fitting parameter in these analyses. As shown in Figures 5–9, data generated from the SPM with chemical reaction at the phase boundary controlling the overall rate fits the experimental data better than the data generated from the SCM with diffusion controlling the overall reaction rate. Therefore we can say that chemical reaction at the phase boundary is the most likely mechanism for all the reactions in this study.

Figure 5. Modeling results for $\text{MgH}_2 + 4 \text{ mol\% CeO}_2$.

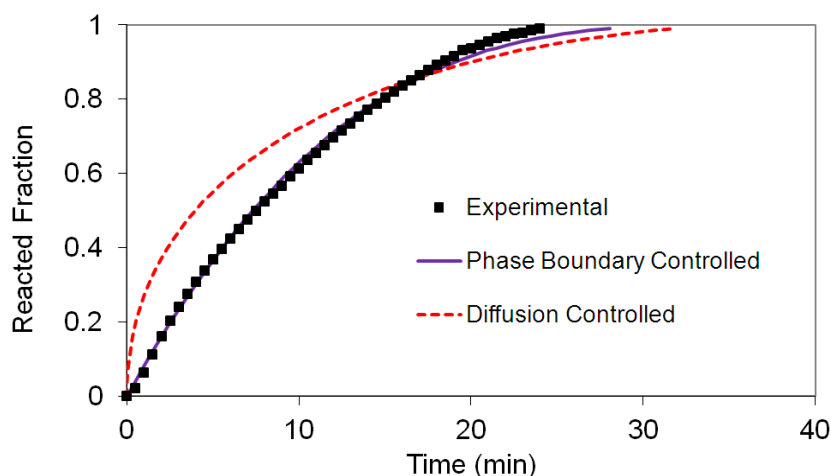


Figure 6. Modeling results for $\text{MgH}_2 + 4 \text{ mol\% Nb}_2\text{O}_5$.

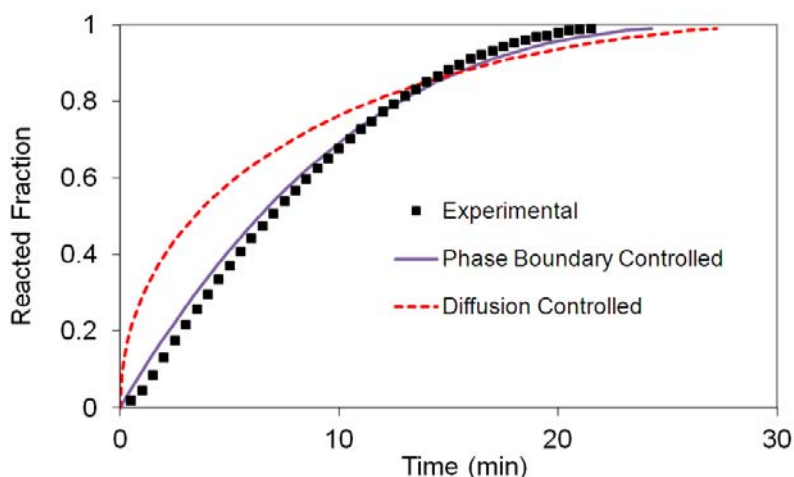
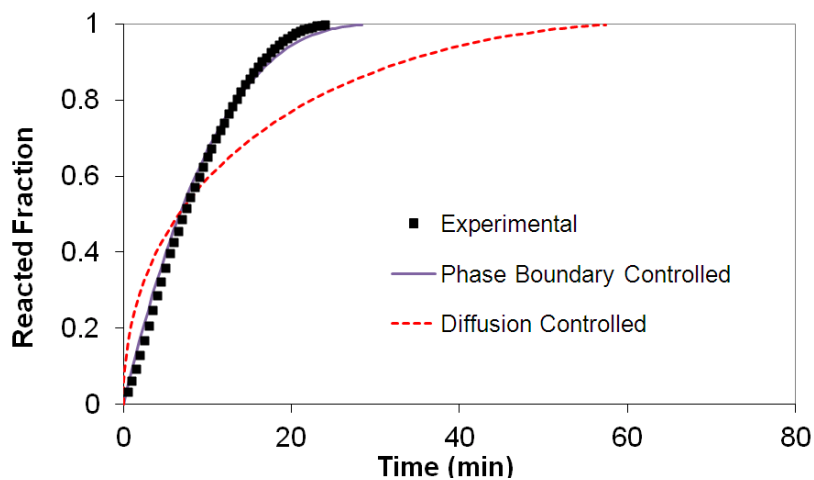
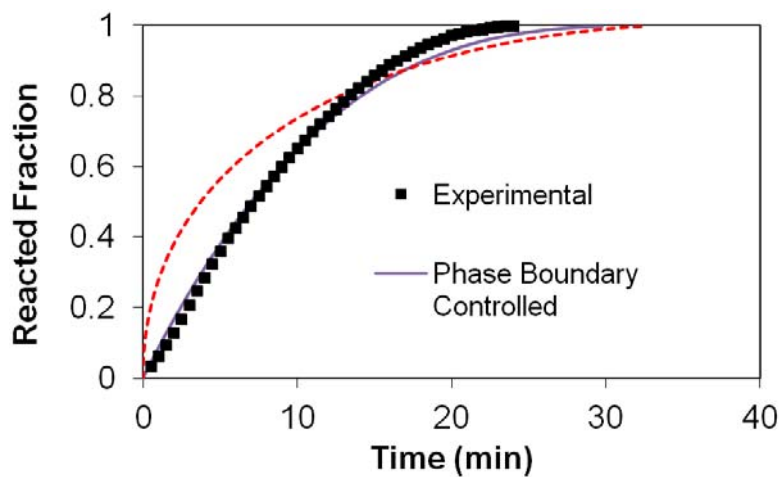
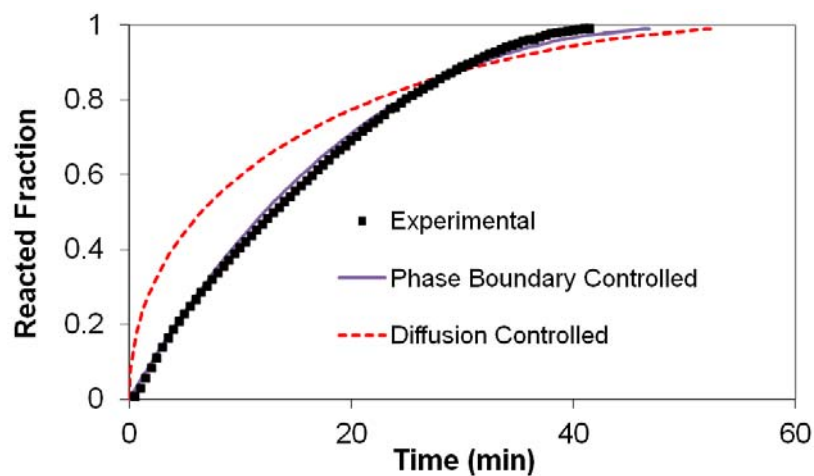


Figure 7. Modeling results for $\text{MgH}_2 + 4 \text{ mol\% ZrO}_2$.**Figure 8.** Modeling results for $\text{MgH}_2 + 4 \text{ mol\% Fe}_3\text{O}_4$.**Figure 9.** Modeling results for MgH_2 .

3.5. Differential Thermal Analysis and Kissinger Plots

To further understand the effects of the transition metal oxide catalysts on the dehydrogenation of MgH_2 , the activation energy of dehydrogenation for the systems studied were investigated using an isoconversion method based on the Kissinger Equation stated below.

$$\ln\left(\frac{\beta}{T_{\max}^2}\right) = -\frac{E_a}{R}\left(\frac{1}{T_{\max}}\right) + F_{\text{KAS}}(\alpha) \quad (3)$$

where T_{\max} is the temperature at maximum reaction rate, β the heating rate, E_a the activation energy, α the fraction of transformation, $F_{\text{KAS}}(\alpha)$ a function of the fraction of transformation, and R is the gas constant. Figure 10 shows the DTA curves for one of the samples ($\text{MgH}_2 + 4 \text{ mol\% Nb}_2\text{O}_5$) at different heating rates from 1 to 15 °C per minute. The figure shows that the endothermic peak corresponding to the maximum rate of dehydrogenation shifts to higher temperatures as the heating rate is increased. The same trend was observed in all the other samples. The plots based on the Kissinger equation are shown in Figure 11. A good linear relationship between $\ln(\beta/T_{\max}^2)$ versus $1/T_{\max}$ existed for all the samples. Activation energies of dehydrogenation were calculated from the slopes of the straight lines. The calculated activation energies are summarized in Table 1. From the values it is clear that the addition of transition metal oxide catalysts to MgH_2 helped lower its activation energy. The calculated activation energies correlate well with the times required for 90% of the hydrogen to desorb from the samples (T_{90}). Lower activation energies correspond to faster desorption kinetics. There was also a slight correlation between the activation energy and desorption temperatures as well. Samples with high activation energies tended to have high thermal stabilities.

Figure 10. Differential Thermal Analysis (DTA) curves for $\text{MgH}_2 + 4 \text{ mol\% Nb}_2\text{O}_5$ at heating rates of 1, 4, 10 and 15 °C/min.

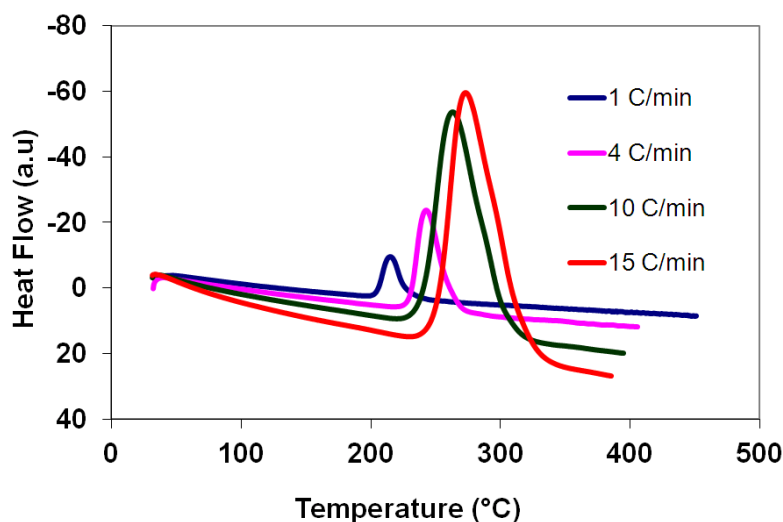
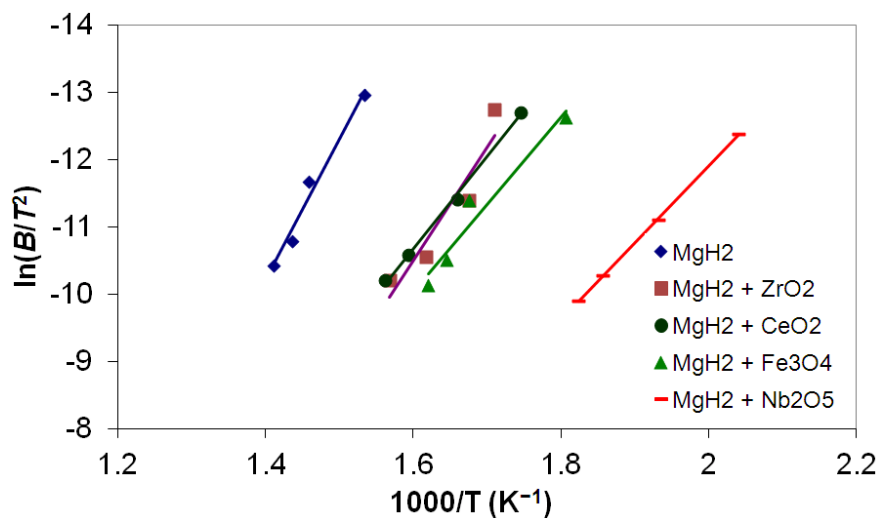


Figure 11. Kissinger plot for MgH₂ and catalyzed MgH₂ materials.

4. Conclusions

This study has shown that transition metal oxide catalysts are effective catalysts for lowering the reaction temperature and increasing the reaction rates of MgH₂. The dehydrodring rates of MgH₂ mixed with transition metal oxide metals were in the order Nb₂O₅ > Fe₃O₄ > CeO₂ > ZrO₂ > pure MgH₂. The mixtures with Nb₂O₅ and Fe₃O₄ both have the lowest desorption temperatures as well as the fastest kinetics although the mixture with Nb₂O₅ has a slight advantage. As seen in Table 1, the mixtures with the fastest reaction times also had the lowest activation energies and ΔH values. Modeling studies show that reaction at the phase boundary is the mechanism controlling the reaction rates in all the reaction mixtures.

Acknowledgments

This work was financially supported by grants from the Department of Energy and the U.S. Department of Transportation.

Conflict of Interest

The authors declare no conflict of interest.

References

1. Sabitu, S.T.; Gallo, G.; Goudy, A.J. Effect of TiH₂ and Mg₂Ni additives on the hydrogen storage properties of magnesium hydride. *J. Alloys Comp.* **2010**, *499*, 35–38.
2. Sabitu, S.T.; Fagbami, O.; Goudy, A.J. Kinetics and modeling study of magnesium hydride with various additives at constant pressure thermodynamic forces. *J. Alloys Comp.* **2011**, *509*, S588–S591.
3. Yang, W.N.; Shang, C.X.; Guo, Z.X. Site density effect of Ni particles on hydrogen desorption of MgH₂. *Int. J. Hydrogen Energy* **2010**, *35*, 4534–4542.

4. Hanada, N.; Ichikawa, T.; Fujii, H. Catalytic effect of Ni nano-particle and Nb oxide on H-desorption properties in MgH₂ prepared by ball milling. *J. Alloys Comp.* **2005**, *404–406*, 716–719.
5. Aguey-Zinsou, K.-F.; Ares-Fernandez, J.R.; Klassen, T.; Bormann, R. Effect of Nb₂O₅ on MgH₂ properties during mechanical milling. *Int. J. Hydrogen Energy* **2007**, *32*, 2400–2407.
6. Hanada, N.; Ichikawa, T.; Hino, S.; Fujii, H. Remarkable improvement of hydrogen sorption kinetics in magnesium catalyzed by Nb₂O₅. *J. Alloys Comp.* **2006**, *420*, 46–49.
7. Evard, E.; Gabis, I.; Yartys, V.A. Kinetics of hydrogen evolution from MgH₂: Experimental studies, mechanism and modeling. *Int. J. Hydrogen Energy* **2010**, *35*, 9060–9069.
8. Luo, Y.; Wang, P.; Ma, L.; Cheng, H. Hydrogen sorption kinetics of MgH₂ catalyzed with NbF₅. *J. Alloys Comp.* **2008**, *453*, 138–142.
9. Barkhordarian, G.; Klassen, T.; Bormann, R. Effect of Nb₂O₅ content on hydrogen reaction kinetics of Mg. *J. Alloys Comp.* **2004**, *364*, 242–246.
10. Jain, I.P.; Lal, C.; Jain, A. Hydrogen storage in Mg: A most promising material. *Int. J. Hydrogen Energy* **2010**, *35*, 5133–5144.
11. Sohn, H.Y.; Emami, S. Kinetics of dehydrogenation of the Mg-Ti-H hydrogen storage system. *Int. J. Hydrogen Energy* **2011**, *36*, 8344–8350.
12. Oelerich, W.; Klassen, T.; Bormann, R. Metal oxides as catalysts for improved hydrogen sorption in nanocrystalline Mg-based materials. *J. Alloys Comp.* **2001**, *315*, 237–242.
13. Koh, J.T.; Goudy, A.J.; Huang, P.; Zhou, J. A comparison of the hydriding and dehydriding kinetics of LaNi₅ hydride. *J. Less-Common Metals* **1989**, *153*, 89–100.
14. Zhang, W.; Cimato, J.; Goudy, A.J. The hydriding and dehydriding kinetics of some LaNi_{5-x}Al_x alloys. *J. Alloys Comp.* **1993**, *201*, 175–179.
15. Smith, G.; Goudy, A.J. Thermodynamics, kinetics and modeling studies of LaNi_{5-x}Co_x hydride system. *J. Alloys Comp.* **2001**, *316*, 93–98.
16. Yang, H.; Ojo, A.; Ogaro, P.; Goudy, A.J. Hydriding and dehydriding kinetics of sodium alanate at constant pressure thermodynamic driving forces. *J. Phys. Chem. C* **2009**, *113*, 14512–14517.
17. Ibikunle, A.; Goudy, A.J.; Yang, H. Hydrogen storage in a CaH₂/LiBH₄ destabilized metal hydride system. *J. Alloys Comp.* **2009**, *475*, 110–115.
18. Durojaiye, T.; Goudy, A.J. Desorption kinetics of lithium amide/magnesium hydride systems at constant pressure thermodynamic driving forces. *Int. J. Hydrogen Energy* **2012**, *37*, 3298–3304.